PAPER

Check for updates

Rational construction of luminescent Eu-doped Y-MOF for ratiometric temperature sensing†

Wei Wei, [ID] * Xi Li, Yong-Ya Zhang [ID] and Jian-Wei Zhang [ID] *

Introducing lanthanide(III) ions into a MOF structure is one of the most effective strategies to construct luminescent MOFs with multiple emission centers for fluorescent applications. In this work, a functionalized Eu^{3+}-doped Y-MOF (Eu@SNNU-325) was constructed by using a cation exchange strategy. The photoluminescence result shows that Eu@SNNU-325 exhibits a unique emission spectrum, namely, the absence of the organic ligand peak and the very strong Y^{3+}/Eu^{3+} characteristic peaks. Interestingly, the smart luminescent Eu@SNNU-325 as a ratiometric thermometer for temperature sensing has good self-calibrated ability and a high maximum relative sensitivity (S_m) value (1.2% K^{-1} at 260 K). This work presents the construction of a smart Eu^{3+}-functionalized Y-MOF thermometer through a cation exchange strategy, providing a good idea for the future development and design of Y-MOF thermometers.

Introduction

Luminescent metal–organic frameworks (LMOFs), as an important class of materials, have advantages for application in light-emitting diodes (LEDs), fluorescent sensors, and bio-imaging, *etc.*[1–15] Generally, most luminescent MOFs with single emission centers exhibit many disadvantages, such as low sensitivity, poor accuracy, and low responsiveness, which limits their widespread application.[16–20] It is well known that the luminescent MOFs with lanthanide ions centers have attracted much research interest owing to their designability, high sensitivity, fast response, and high accuracy.[21–23] Therefore, the rational design of lanthanide ions based-MOFs (Ln-MOFs) is still a great challenge.

In recent years, the luminescent Ln-MOF thermometers have been widely studied due to their distinct characteristic emissions, wide temperature detection range and strong anti-interference abilities.[24–30] On the other hand, when constructing Ln-MOFs, selecting appropriate organic ligands as antenna chromophores plays a key role in sensitizing Ln^{3+} ion emissions. However, MOF materials based on rare earth Y^{3+} ions are still rare.

To our knowledge, a highly ultra-stable yttrium-MOF (SNNU-325, SNNU = Shaanxi Normal University) consists of the Y^{3+} ions, π-conjugated ligands, large octahedral cages, and quadrilateral channels, which can be potentially applied in the field of fluorescence sensing.[31] This yttrium-MOF (Y-MOF) has been

School of Chemistry and Chemical Engineering, Shangqiu Normal University, Shangqiu, Henan, 476000, P. R. China. E-mail: weiweizzuli@163.com; jwzhang85@163.com

† Electronic supplementary information (ESI) available. See DOI: https://doi.org/10.1039/d4ra05796a

reported by Zhai's group, and its crystal structure, characterization, and gas adsorption/separation performance have been studied. However, the fluorescence performance of this Y-MOF has not yet been studied. Based on the structural characteristics of SNNU-325, we speculate that this MOF constructed from Y^{3+} ions and rich π-conjugated aromatic ligands should exhibit excellent unique fluorescence properties.

Herein, we have successfully synthesized this Y-MOF (SNNU-325) and further studied its structural characteristics. The result of elemental mappings demonstrates that Sc^{3+} ions are uniformly dispersed on the MOF. The presence of Sc^{3+} ions in the pores provides technical support for introducing lanthanide(III) ions with strong luminescent properties *via* a cation exchange strategy (Scheme 1). More significantly, the luminescent Eu@SNNU-325 as a ratiometric thermometer not only exhibits the Y^{3+}/Eu^{3+} characteristic peaks but also shows good
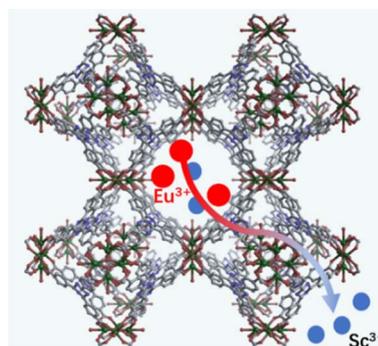
Scheme 1 Schematics illustrating the cation exchange strategy to construct a functionalized Eu-doped Y-MOF.

Paper

fluorescence temperature sensing over a wide range of temperature from 80 K to 260 K.

Experimental

Synthesis of SNNU-325

A mixture of the ligand H_3TATB (2,4,6-tris(4-carboxyphenyl)-1,3,5-triazine) (12 mg, 0.027 mmol), $Y(NO_3)_3\cdot 6H_2O$ (12 mg, 0.03 mmol), $Sc(NO_3)_3\cdot 6H_2O$ (16 mg, 0.07 mmol) and 2-FBA (2-fluorobenzoic acid) (173 mg, 1.23 mmol) was ultrasonically dissolved in DMF (N,N-dimethylformamide) (6 mL)/H_2O (0.9 mL) solvent system in a glass vial (20 mL). The mixed solution was placed in an oven preheated at 90 °C for 5 days and then cooled to room temperature. After that, the colorless cubic block crystals were obtained by filtering and washing the fresh DMF and EtOH, and then dried at 50 °C.

Synthesis of Eu@SNNU-325

The above obtained Y-MOF (50 mg) and $EuCl_3\cdot 6H_2O$ (50 mg) were dispersed in DMF (5 mL) and then placed in an oven at 75 °C for 24 h. The obtained Eu@SNNU-325 sample was obtained by washing several times with fresh DMF and then dried in an oven at 50 °C.

Results and discussion

Characterizations of SNNU-325 and Eu@SNNU-325

The preparation of SNNU-325 was reported in the literature.[31] The PXRD peaks of as-synthesized SNNU-325 are in good agreement with the simulated peaks from the crystal structure data (Fig. 1). The author pointed out in the original paper that SNNU-325 cannot be prepared without the addition of $Sc(NO_3)_3\cdot 6H_2O$. After careful analysis of this Y-MOF structure, we speculate that Sc^{3+} ions not only play a structural guiding role in the formation of MOF and but also as cations exist within the MOF framework. To prove our hypothesis, we first soaked the as-synthesized Y-MOF in methanol for 4 days, and then conducted EDS testing on the as-synthesized and the methanol-treated sample, respectively (Fig. S1 and S2†). The EDS results
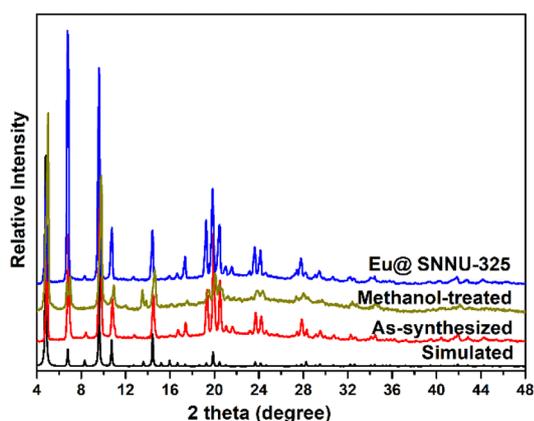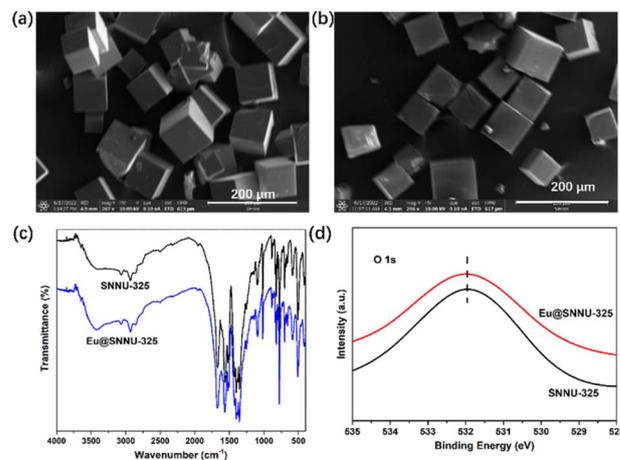

Fig. 2 SEM images of SNNU-325 (a) and Eu@SNNU-325 (b). (c) FT-IR spectra of SNNU-325 and Eu@ SNNU-325. (d) The O 1s XPS spectra of SNNU-325 and Eu@ SNNU-325.

show that the atomic ratios of Sc/Y significantly decrease from 1.99 to 0.35 in the as-synthesized sample and the methanol-treated sample. The PXRD peaks of the methanol-treated sample are well-matched with the as-synthesized sample
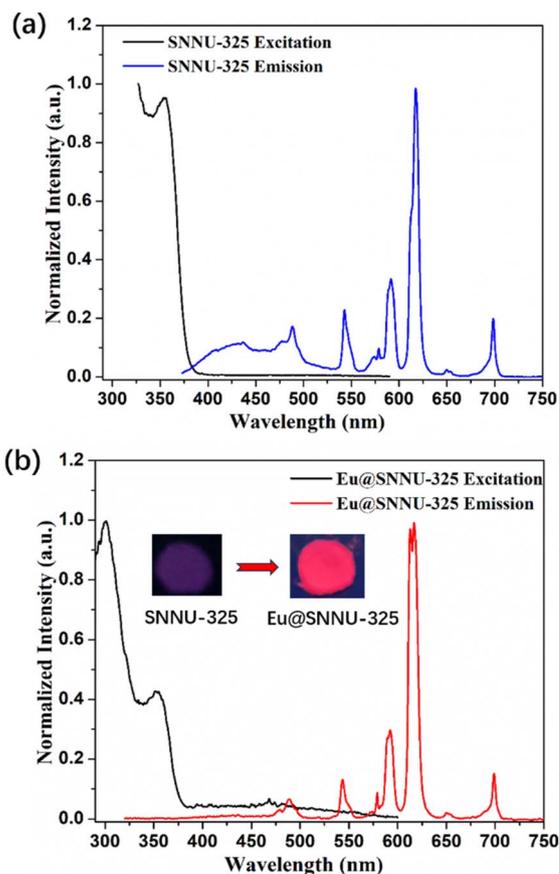

Fig. 3 Excitation and emission spectra of SNNU-325 (λ_{ex} = 353 nm) (a) and Eu@SNNU-325 (λ_{ex} = 300 nm) (b) (insets show the photographs under 254 nm UV light).

Fig. 1 PXRD patterns of the simulated, as-synthesized SNNU-325, methanol-treated SNNU-325 and Eu@SNNU-325.
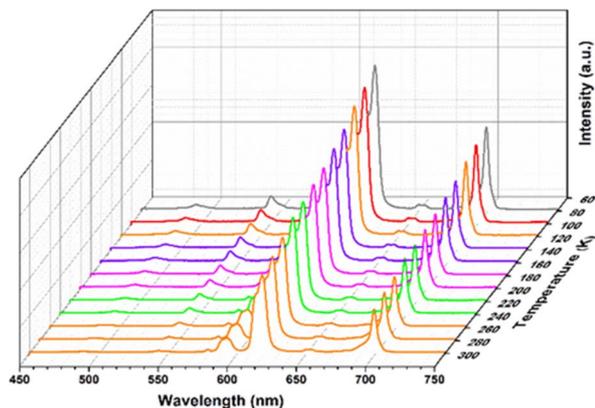
Fig. 4 Temperature-dependent emission spectra of Eu@SNNU-325 recorded in the range of 80–300 K.
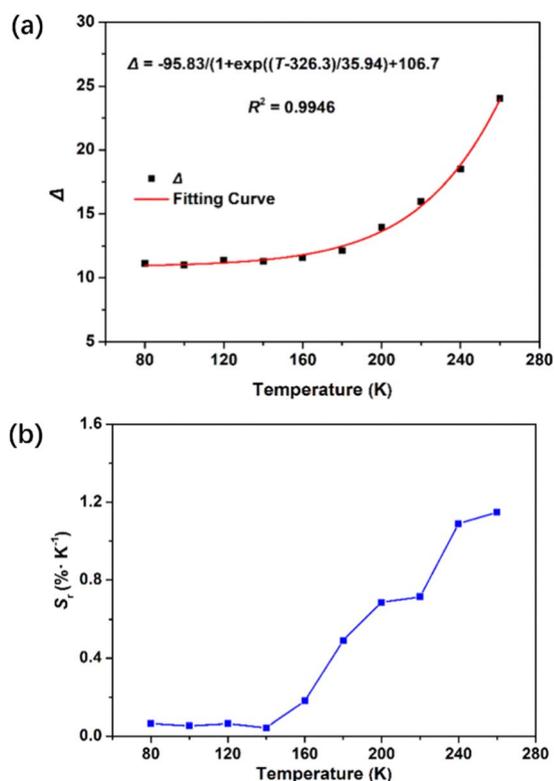

Fig. 5 (a) Temperature-dependent emission intensity ratio Δ (I_{618}/I_{544}) and the fitted curve of Eu@SNNU-325 from 80 to 260 K. (b) Temperature-dependent relative sensitivity (S_r) of Eu@SNNU-325.

(Fig. 1). Through the methanol-treated sample for 4 days, it can be clearly observed that the Sc^{3+} ions only decrease in the MOF framework, but cannot be completely removed. This phenomenon indicates that there is a strong interaction force between Sc^{3+} ions within the MOF framework. Therefore, the presence of Sc^{3+} ions within the MOF framework encourages us to design Eu^{3+} doped Y-MOFs by using a cation exchange strategy.

The mixture of as-synthesized Y-MOF and $EuCl_3 \cdot 6H_2O$ under DMF solvent was further employed to construct Eu-

functionalized Y-MOFs by post-synthetic modification strategy. By comparing the powder X-ray diffraction (PXRD) peaks (Fig. 1), the peaks of Eu@SNNU-325 remain highly consistent with that of the as-synthesized sample, indicating that this Y-MOF still maintains its crystalline structure after the incorporation of Eu^{3+} ions into the framework. As shown in Fig. 2a and b, the SEM images show that the morphologies of Eu^{3+} remain consistent before and after being introduced into the MOF framework. The elemental mapping images clearly show the homogeneous distribution of C, N, O, F, Cl, Y, Sc and Eu elements in the Eu@SNNU-325 (Fig. S3†), indicating that the Eu^{3+} ions were incorporated into the MOF framework through the Sc^{3+} ions exchange process. Notably, the presence of F or Cl elements in the Eu@SNNU-325 are originated from the raw materials (2-FBA and $EuCl_3 \cdot 6H_2O$). Moreover, the FT-IR spectra of SNNU-325 and Eu@SNNU-325 are basically consistent, further indicating that the incorporation of Eu^{3+} ions not change the original structure (Fig. 2c). To demonstrate whether Eu^{3+} has exchanged Y^{3+} ions in the skeleton, X-ray photoelectron spectroscopy (XPS) spectra of SNNU-325 and Eu@SNNU-325 were recorded. The results show that the O 1s XPS spectra of SNNU-325 and Eu@ SNNU-325 remain consistent, indicating that Eu^{3+} ions are not bonded to oxygen atoms in the MOF skeleton, and also indicating that Eu^{3+} ions do not exchange Y^{3+} ions in the skeleton (Fig. 2d).

Photoluminescence study

Considering the unique Y^{3+} ion characteristic, rich π-conjugated organic ligand, and the very obvious Eu^{3+} emission bands, we measured the solid-state photoluminescence (PL) spectra of SNNU-325 and Eu@SNNU-325 at room temperature. As shown in Fig. 3a, the emission spectrum of SNNU-325 shows two characteristic emission centers ($\lambda_{ex} = 355$ nm), one at 435 nm belonging to ligand emission,[32] and the other at 488, 544, 578, 592, 618, 651 and 699 nm belonging to Y^{3+} ion characteristic emission.[33] However, the emission spectrum of Eu@SNNU-325 is consistent with that of SNNU-325, except for the disappearance of the emission peak of the $TATB^{3-}$ ligand ($\lambda_{ex} = 300$ nm) (Fig. 3b). It can be clearly observed that the absence of the emission band (at about 435 nm) arising from the ligand, indicating that the ligand emission process in Eu@SNNU-325 should be suppressed by the energy transfer from the ligand to the Eu^{3+} and Y^{3+} ions.[34,35] Under UV-light irradiation, SNNU-325 displays dark purple visible emission, and Eu@SNNU-325 displays red visible emission (insets in Fig. 3b). The above results demonstrate that the emission spectrum of Eu^{3+} doped Y-MOFs has not changed compared to that of Y-MOF, but affect the energy transfer between the organic ligand and Eu^{3+} and Y^{3+} ions, resulting in Eu@MOF displaying strong red emission of Eu^{3+}. This phenomenon is very rare in other Eu^{3+}-doped MOF systems.

Temperature-dependent emission properties

The significant luminescence characteristics of Y^{3+}/Eu^{3+} ions in the Eu@SNNU-325 inspired us to evaluate its application in the field of low-temperature sensing. The temperature-dependent

fluorescence performance of Eu@SNNU-325 was studied over a wide range of temperature from 80 K to 300 K. As shown in Fig. 4, the luminescence intensities in the Eu@SNNU-325 gradually decrease of both I_{618} and I_{544} with the increasing temperature under excitation at 300 nm, which can be mainly attributed to the thermal deactivation of the Y^{3+}/Eu^{3+} ions. As a ratiometric luminescent thermometer, the intensity ratio of I_{618}/I_{544} (Δ) of Eu@SNNU-325 was used to evaluate its temperature sensing performance. The Boltzmann equation ($\Delta = (A_1 - A_2)/(1 + \exp((T - T_0)/dT)) + A_2$) was used to fit the relationship between Δ and the a wide temperature range (80–260 K). Interestingly, the result shows that Eu@SNNU-325 exhibits a good fit ($R^2 = 0.9946$) (Fig. 5a, and Table S1†).

To further evaluate the sensing sensitivity, the relative sensitivity (S_r, $S_r = |(\partial\Delta/\partial T)/\Delta|$) was used as an important index. Because S_r represents an intrinsic nature of the thermometer. As a result, the maximum relative sensitivity (S_m) was determined to be 1.2% K^{-1} at 260 K (Fig. 5b), which was comparable to that of the other reported luminescent MOF thermometers such as $Tb_{0.80}Eu_{0.20}$(bpda) (1.39),[36] ZJU-88⊃perylene (1.28)[37] and $Nd_{0.577}Yb_{0.423}$BDC-F_4 (1.2).[38] The above results show that Eu@SNNU-325 can be used as a smart thermometer for self-calibrating temperature sensing.

Conclusions

In summary, a functionalized Eu-doped Y-MOF (Eu@SNNU-325) has been constructed by the cation exchange strategy. The obtained Eu@SNNU-325 was characterized by combining the PXRD, SEM, XPS, FT-IR, and EDX mapping. Due to the introduction of Eu^{3+} ions into the Y-MOF framework, Eu@SNNU-325 exhibits the characteristic emission centers of Y^{3+}/Eu^{3+} ions. Moreover, the smart luminescent Eu@SNNU-325 exhibits highly sensitive temperature sensing over a wide range of temperature from 80 K to 260 K. Most importantly, the maximum relative sensitivity (S_m) of Eu@SNNU-325 reached 1.2% K^{-1} at 260 K, indicating that it can be applied as a temperature transfer material in practical applications. This work provides a powerful and effective synthesis strategy for constructing Eu-doped Y-MOFs and applying a field of fluorescence temperature sensing.

Data availability

Data are available upon request from the authors.

Author contributions

Wei Wei: experiment instruction, methodology. Xi Li: data curation. Yong-Ya Zhang: software. Jian-Wei Zhang: writing – review and editing.

Conflicts of interest

There are no conflicts to declare.

Acknowledgements

References

1 Y. Cui, Y. Yue, G. Qian and B. Chen, *Chem. Rev.*, 2012, **112**, 1126–1162.

2 B. Li, H.-T. Fan, S.-Q. Zang, H.-Y. Li and L.-Y. Wang, *Coord. Chem. Rev.*, 2018, **377**, 307–329.

3 E. J. McLaurin, L. R. Bradshaw and D. R. Gamelin, *Chem. Mater.*, 2013, **25**, 1283–1292.

4 A. Karmakar and J. Li, *Chem. Commun.*, 2022, **58**, 10768–10788.

5 G.-H. Wen, X.-M. Chen, K. Xu, X. Xie, S.-S. Bao and L.-M. Zheng, *Dalton Trans.*, 2021, **50**, 17129–17139.

6 J. Dong, D. Zhao, Y. Lu and W.-Y. Sun, *J. Mater. Chem. A*, 2019, **7**, 22744–22767.

7 S. Bhowal and A. Ghosh, *RSC Adv.*, 2021, **11**, 27787–27800.

8 S.-Y. Li, X. Yan, J. Lei, W.-J. Ji, S.-C. Fan, P. Zhang and Q.-G. Zhai, *ACS Appl. Mater. Interfaces*, 2022, **14**, 55997–56006.

9 Z. Hu, B. J. Deibert and J. Li, *Chem. Soc. Rev.*, 2014, **43**, 5815–5840.

10 Y. Zhang, S. Yuan, G. Day, X. Wang, X. Yang and H.-C. Zhou, *Coord. Chem. Rev.*, 2018, **354**, 28–45.

11 G.-L. Yang, X.-L. Jiang, H. Xu and B. Zhao, *Small*, 2021, **17**, 2005327.

12 Y. Liu, X.-Y. Xie, C. Cheng, Z.-S. Shao and H.-S. Wang, *J. Mater. Chem. C*, 2019, **7**, 10743–10763.

13 M. Ding, R. W. Flaig, H.-L. Jiang and O. M. Yaghi, *Chem. Soc. Rev.*, 2019, **48**, 2783–2828.

14 Y. Cui, B. Li, H. He, W. Zhou, B. Chen and G. Qian, *Acc. Chem. Res.*, 2016, **49**, 483–493.

15 D. Yue, Z. Li, D. Chen, W. Li, B. Qin, B. Zhang, Y. Li, D. Zhao and Z. Wang, *J. Solid State Chem.*, 2023, **327**, 124279.

16 Z.-H. Zhu, Z. Ni, H.-H. Zou, G. Feng and B. Z. Tang, *Adv. Funct. Mater.*, 2021, **31**, 2106925.

17 Z.-J. Li, X. Wang, L. Zhu, Y. Ju, Z. Wang, Q. Zhao, Z.-H. Zhang, T. Duan, Y. Qian, J.-Q. Wang and J. Lin, *Inorg. Chem.*, 2022, **61**, 7467–7476.

18 E. Velasco, G. Zhang, S. J. Teat, K. Tan, S. Ullah, T. Thonhauser and J. Li, *Inorg. Chem.*, 2023, **62**, 16435–16442.

19 C. Yao, Y. Xu and Z. Xia, *J. Mater. Chem. C*, 2018, **6**, 4396–4399.

20 C. Yang, X. Xu and B. Yan, *Inorg. Chem. Front.*, 2023, **10**, 2951–2960.

21 S. Wu, H. Min, W. Shi and P. Cheng, *Adv. Mater.*, 2020, **32**, 1805871.

22 H.-Q. Yin and X.-B. Yin, *Acc. Chem. Res.*, 2020, **53**, 485–495.

23 Y.-M. Wang, X.-T. Tian, H. Zhang, Z.-R. Yang and X.-B. Yin, *ACS Appl. Mater. Interfaces*, 2018, **10**, 22445–22452.

24 Y. Yang, Y. Wang, Y. Feng, X. Song, C. Cao, G. Zhang and W. Liu, *Talanta*, 2020, **208**, 120354.

25 K. Li, D. Mei and B. Yan, *Chem. Eng. J.*, 2023, **475**, 146380.

26 L. Li, J.-Y. Zou, S.-Y. You and L. Zhang, *Inorg. Chem.*, 2023, **62**, 14168–14179.

27 C. Hong, L. Li, J.-Y. Zou, S.-Y. You, E.-L. Wang, L. Zhang, Y.-W. Liu and Y.-L. Huang, *Inorg. Chem.*, 2024, **63**, 4697–4706.

28 E.-L. Wang, L. Li, J.-Y. Zou, C. Hong, L. Zhang and S.-Y. You, *ACS Appl. Nano Mater.*, 2024, **7**, 17748–17758.

29 T. Xia, J. Wang, K. Jiang, Y. Cui, Y. Yang and G. Qian, *Chin. Chem. Lett.*, 2018, **29**, 861–864.

30 S. Xing and C. Janiak, *Chem. Commun.*, 2020, **56**, 12290–12306.

31 J. Lei, P. Zhang, Y.-Y. Xue, J. Xu, H.-P. Li, H.-J. Lv, Y. Wang, S.-N. Li and Q.-G. Zhai, *Sep. Purif. Technol.*, 2022, **283**, 120211.

32 J.-W. Zhang, X. Li, Y.-Y. Zhang and X.-C. Hu, *J. Mol. Struct.*, 2024, **1309**, 138154.

33 D.-P. Li, F. Wang, Y. Tian, S.-M. Liu, D.-C. Liu, B. Yang and B.-Q. Xu, *Opt. Mater.*, 2020, **108**, 109757.

34 Y.-J. Chen, C.-X. Dou, P.-P. Yin, J.-T. Chen, X.-G. Yang, B. Li, L.-F. Ma and L.-Y. Wang, *Dalton Trans.*, 2023, **52**, 13872–13877.

35 R. He, Y.-L. Wang, H.-F. Ma, S.-G. Yin and Q.-Y. Liu, *Dyes Pigm.*, 2018, **151**, 342–347.

36 D. Zhao, X. Rao, J. Yu, Y. Cui, Y. Yang and G. Qian, *Inorg. Chem.*, 2015, **54**, 11193–11199.

37 Y. Cui, R. Song, J. Yu, M. Liu, Z. Wang, C. Wu, Y. Yang, Z. Wang, B. Chen and G. Qian, *Adv. Mater.*, 2015, **27**, 1420–1425.

38 X. Lian, D. Zhao, Y. Cui, Y. Yang and G. Qian, *Chem. Commun.*, 2015, **51**, 17676–17679.